Acoustic Detection and Classification of Fluid-filled Cylinders Embedded in Sediments

B. Woodward B and P.A. Lepper
Department of Electronic and Electrical Engineering
Loughborough University
Loughborough, LE11 3TU, United Kingdom
b.woodward1@lboro.ac.uk

***Abstract*-An open-water trial was carried out using a parametric sonar system with the aim of detecting and classifying embedded or partially embedded objects such as pipelines, lost cargo and mines. This was a contribution to the European Commission's MAST-III DEO (Detection of Embedded Objects) project. The trial involved the detection of back-scattered signals from a water-filled, thin-walled steel cylinder with flat end-caps. Comparisons of incident and back-scattered signals were made at both the 'primary' frequency of 75 kHz and at 'secondary' frequencies in the range 1-13 kHz for sine wave, chirp and Ricker pulses. The main finding was that both specular reflections and resonance effects could be observed and it is proposed that these could contribute to the classification of targets.**

I. INTRODUCTION

There has been considerable interest in the detection and characterisation, or classification, of objects buried in underwater sediments [1-5]. The aim of this research was to attempt to detect and classify a partially embedded object by analysing back-scattered signals, using a parametric sonar system as an acoustic source [2,5]. The system, which was developed for both sediment characterisation and for the detection and classification of buried objects, operates at a 'primary' frequency of 75 kHz and generates 'secondary' frequencies in the range 1-13 kHz. Its highly directional beam (2.5º in both azimuth and elevation) can penetrate sediments to a depth of several metres. The object ('target') was a closed steel cylinder (1m long, 0.25m diameter, 6mm wall thickness) resting proud of the seabed on soft sediment in a depth of 40-45m, depending on the tide. Measurements were made at various source-target aspect angles and seabed grazing angles using a variety of signal types. Only a water-filled target was considered, due to the difficulty of sinking an air-filled target. Recordings of target-scattered signals were made using single-element hydrophones for both primary signals and secondary signals.

A sea trial took place on Loch Duich, Scotland in collaboration with TNO, The Netherlands, using a raft and other facilities of the Scottish Fisheries Research Service (FRS). The paper outlines the equipment deployed, the method used to obtain experimental data and finally the data analysis and results. Some examples serve to illustrate how signal analysis can yield information about the physical dimensions, and hence the classification, of an embedded target.

II. EQUIPMENT

The trial equipment was deployed as shown in Fig. 1. The Loughborough University (LU) parametric array was mounted on a pan-and-tilt assembly below the FRS raft and the target was suspended beneath a second raft. Both rafts were held in place by a pair of anchored 'tram line' wires so that the source-target separation could be varied. The transmission elevation angle could be varied over a range of $\pm 20^0$ using the pan-and-tilt and the azimuth angle could be varied over a range of $\pm 18^0$ by electronically steering the array's beam. The array was initially deployed at 10m depth to limit the cavitation caused by operation at high power, which was up to 1 kW per stave, or 13 kW in total. The depth of the array could be adjusted to provide different seabed grazing angles for a target in a fixed position.

A streamer array was deployed from the FRS raft by TNO-FEL, as shown in Figs 1 and 2, but this will not be described here because data obtained with it are not presented.

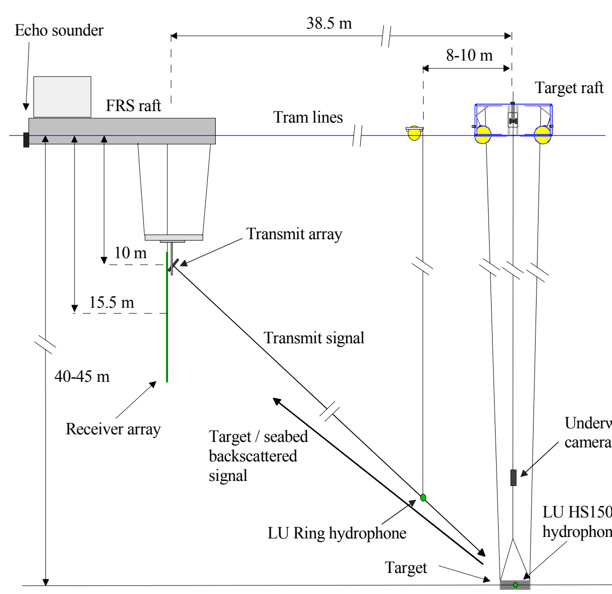

Fig. 1. Equipment deployment.

0-933957-31-9

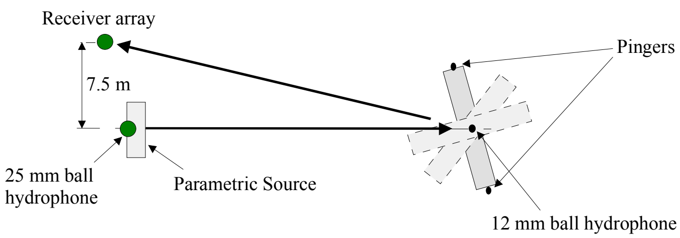

Fig. 2. Target aspect angle measurement using pingers.

Three single-element hydrophones were deployed for the purpose of signal monitoring; these were:

- *H_1, 10cm-diameter ring* (Sonar Products Ltd): Attached to a 100-metre cable, this hydrophone was placed in the array's beam at a distance of typically 10-15m from the target. The ring provided good low-frequency receive sensitivity (1-15 kHz) with a peak of –181 dB re 1V/µPa at 11 kHz. It was used to detect direct signals and target/seabed back-scattered signals.
- *H_2, 12mm ball* (SRD Ltd, HS150): This hydrophone, with a resonant frequency close to 150 kHz, was placed at the geometrical centre of the flooded cylindrical target on the seabed. It was used to detect high-frequency primary signals during source-target alignment and had a calibrated receive sensitivity of -217 dB re 1V/µPa.
- *H_3, 25mm ball* (SRD Ltd, HS70): This hydrophone, with a resonant frequency close to 70 kHz, was deployed from the FRS raft near the parametric array, as shown in plan view in Fig. 2. It was used to detect high-frequency signals from two pingers placed inside the cylindrical target, thereby allowing a measure of target orientation, as explained later.

The hydrophones were monitored using a Tektronix 420 TDS digital oscilloscope and the LU data capture system [1,2], which provided real-time frequency and time domain analysis. An underwater camera was deployed from the target raft to observe the aspect angle and degree of embedding.

Improved communications between the FRS raft and the TNO base station ashore 500 metres away were achieved using Desklink software. With a 1-km fibre-optic link, a local area network (LAN) enabled a raft-based computer to be remotely operated from the TNO base.

III. SET-UP METHODS

Once the target was resting on the seabed, two set-up procedures were necessary before experimental data could be obtained. Figs 1 and 2 illustrate the geometry of the experimental set-up. The first procedure was to align the parametric array beam with the target, and hence to estimate the grazing angle, i.e. the angle between array's transmission axis and the seabed, since this is a necessary classification parameter. Also, alignment ensured that maximum acoustic energy was incident on the target. The method used was to adjust the array's azimuth and elevation angles while observing the signal from hydrophone H_2 placed at the centre of the target, which was initially aligned as closely as possible in a broadside aspect. When a peak signal level was observed, correct alignment was achieved.

The second procedure was to measure the source-target aspect angle, i.e. the angle between the transmission axis and the axis of symmetry of the cylindrical target, which was approximately horizontal. Various aspect angles were achieved by raising, turning and lowering the target on a three-wire suspension system deployed from the target raft. One way of determining the angle was to use two acoustic pingers, placed inside the target and separated from each other by 1m, to measure the phase alignment of the two signals arriving at hydrophone H_3. Each pinger transmitted a 4ms long, 35 kHz continuous wave (CW) signal, first one and then the other after a fixed delay. The time difference could then be measured, with the fixed delay removed, giving the difference in the propagation distances of the two signals. In the broadside aspect the signals should be precisely phase-aligned. Rotation of the target moved one pinger closer to or farther away from H_3, hence altering the propagation distances and correspondingly the signal arrival times. The timing difference could then be translated into a rotation angle [5].

Because of noise problems encountered with the pingers, an underwater video camera was used to check the target aspect angle. Once the target was positioned the camera and lights were lowered on one of the target lifting wires. To measure the target orientation an oil-filled compass was placed in the field of view of the camera. Post-processing of the video images allowed measurement of the aspect angle.

IV. MEASUREMENTS

With the parametric source deployed at 10m depth and at a horizontal range of 38.5 m from the target, the corresponding grazing angles were between about 38^0 and 42^0. The angular variation was due to the change in water depth during the tidal cycle. The target was then deployed at a range of aspect angles. Discrete aspect angles at which measurements were made were -43^0, -42^0, $+33^0$, $+43^0$, $+51^0$, $+77^0$, $+96^0$, $+114^0$, $+83^0$, $+26^0$, $+32^0$ and -4^0. Due to difficulties in exact target placement the closest orientation to broadside (0^0) and end-cap positions ($\pm 90^0$) were -4^0 and $+96^0$ respectively. Measurements were also made to establish the scattering strength of the sediment alone, with the target lifted above the seabed.

Insonification at each target aspect angle was conducted using a variety of transmitted signals:

- 4ms CW tones, at frequencies of 5, 9 and 13 kHz;
- frequency modulated 'chirp' signals, initially over the ranges 2-10 kHz and 4-12 kHz, later replaced by single octave chirps of 3-6 kHz and 6-12 kHz;
- short Ricker pulses, centred on 4, 7 and 10 kHz.

Data for each signal type, and for each target aspect angle, were sampled at 250 kHz and recorded to 16-bit resolution, both for narrow-band (1-25 kHz) and broadband (1-100 kHz) recording.

V. DATA ANALYSIS

Comparison of both direct and target-scattered signals could be made, due to the positioning of the hydrophones. Fig. 3 shows the wide-band recording for a 7 kHz Ricker generation signal, for both the direct signal and the target echoes, at both the primary and secondary frequencies.

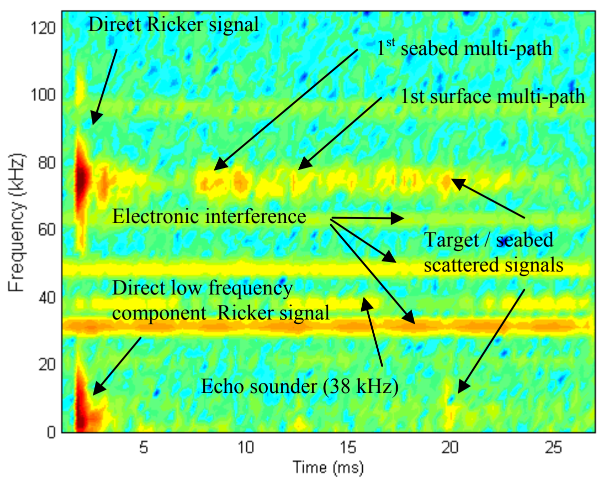

Fig. 3. Broad-band spectrogram for target insonification by 7 kHz Ricker signal: 50^0 grazing angle, -4^0 aspect angle.

This spectrogram was recorded from hydrophone H_1, placed 13.3 m from the target in the beam of the incident signal. The target was at -4^0 from the broadside position and approximately 50 % embedded. The time scale, corresponding to the start of the data capture window, was selected to allow measurement of both the direct and seabed-scattered signals. The capture window started 18 ms after the leading edge of the transmission pulse. The corresponding source-target distance of 43.4m was measured using hydrophone H_2. With a water depth of 43 m, the estimated seabed-grazing angle was 50^0.

Spectral analysis was carried out using a 128-point Fast Fourier Transform (FFT) with a 128-point sliding window. No compensation was made for the hydrophone response at the higher frequencies, but comparison of relative positions in time of the low- and high-frequency components was considered useful. Due to the reduced sensitivity of hydrophone H_1 at 75 kHz, the low and high frequency components of the direct signal appear of similar amplitude. In reality, the approximate 40 dB difference in signal level would tend to make the weaker, lower frequency components harder to distinguish in the display format shown in Fig. 3.

Both the higher frequency component (centred on 75 kHz) and the lower frequency Ricker signals (centred on about 7 kHz) are clearly visible for the direct signal. A strong echo is also visible in both frequency bands in the expected time window for the known target position. The higher frequency signal includes additional echoes, making detection of the target signature harder if the target's position was unknown. The strong return corresponding to the known target position was due to contributions from both the target and from the sediment in the insonified footprint. Comparison with the lower frequency target/seabed echoes, shows a more distinct echo, suggesting that the majority of the back-scattered energy in this band was due to the presence of the target. The more cluttered higher frequency signals are probably due to the higher back-scattering strength of the sediment. The lower frequency component, which was more likely to penetrate the sediment, generated less significant back-scattered energy. Insonification of an embedded object having a much higher target strength than the back-scattering strength of the sediment therefore contributes the majority of the back-scattered energy. These observations were borne out by experiment by making comparisons of spectra obtained with and without the target in place. Assuming a spherical spreading loss of 3.7 dB for the propagation from the target to the hydrophone, the calculated target strength of the embedded cylinder was –34 dB.

Fig. 3 also illustrates the directional properties of the secondary frequency signal, with little or no additional back-scattered signal, compared with the primary frequency signal. The additional back-scattered signal contributions at the higher frequencies were caused by the higher reflectivity and by energy in the side-lobes of the signal. This is evident in the identification of the first seabed and surface multi-path signals detected for this geometry. Little or no indication of multipath components is evident at the lower frequencies.

Fig. 4 shows the narrow-band time domain response of the direct and target/seabed echoes for the target in approximately broadside aspect. The amplitude scale is expanded to enhance the target echo relative to the direct signal, which appears clipped. The response of hydrophone H_1 at the lower frequencies is relatively flat and no compensation for variations in hydrophone sensitivity with frequency was made in the analysis of narrow-band recordings.

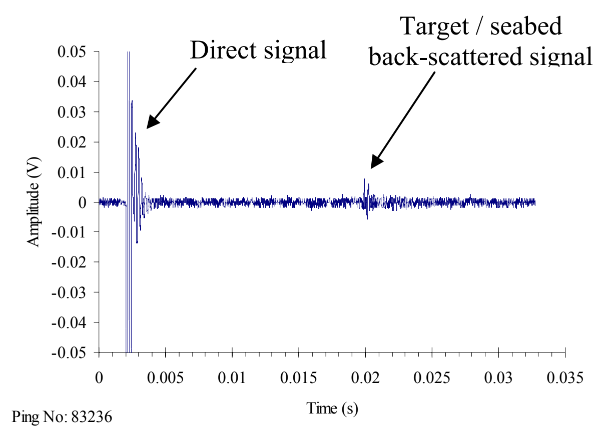

Fig. 4. Direct signal and seabed/target echo for target insonification by 7 kHz Ricker signal: -4^0 aspect angle.

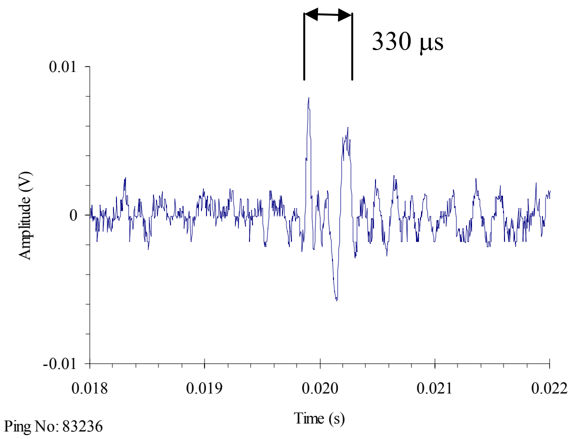

Fig. 5. Expanded seabed/target echo for target insonification by 7 kHz Ricker signal: -4^0 aspect angle.

An expanded view of the seabed/target echo is shown in Fig. 5. The delay of 330 μs between the positive-going peaks again closely matched the through-water propagation distance of 0.495m. This is close to the two-way path across the diameter of the cylinder, suggesting specularly reflected, lower frequency energy from both its front and back faces. Between the two peaks there is evidence of a lower frequency component, which appears to start at the negative-going part of the signal. Further information can be extracted from Figs 6 and 7, showing narrow-band (1-25 kHz) spectra of target-scattered signals observed at seabed grazing angles of 40^0 and 35^0, both for a near-broadside target aspect angle. In each case there is evidence of a front-face specular return at about 6-14 kHz and low frequency resonance effects at about 3-7 kHz. The intensity colour scales were selected arbitrarily to provide the best contrast against the background for each echo.

Fig. 6 shows the target echo contribution for a 7 kHz

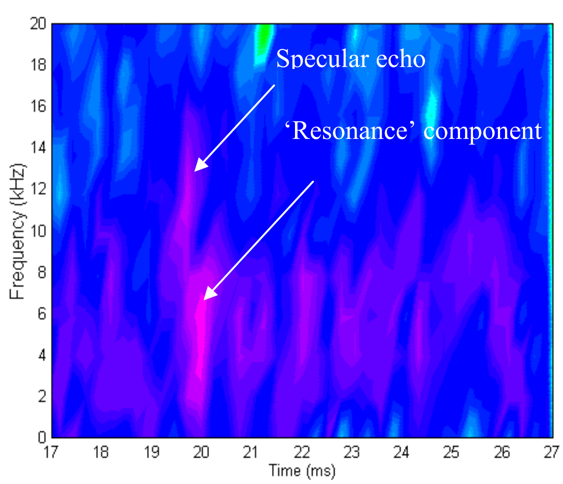

Fig. 6. Narrow-band spectrogram for target insonification by 7 kHz Ricker signal: 40^0 grazing angle, -4^0 aspect angle.

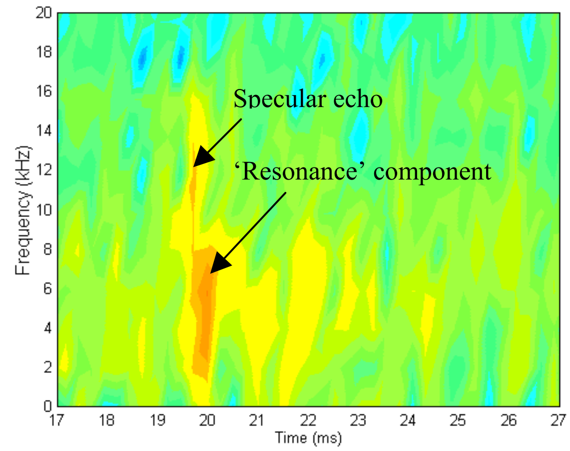

Fig. 7. Narrow-band spectrogram for target insonification by 7 kHz Ricker signal: 35^0 grazing angle, -4^0 aspect angle.

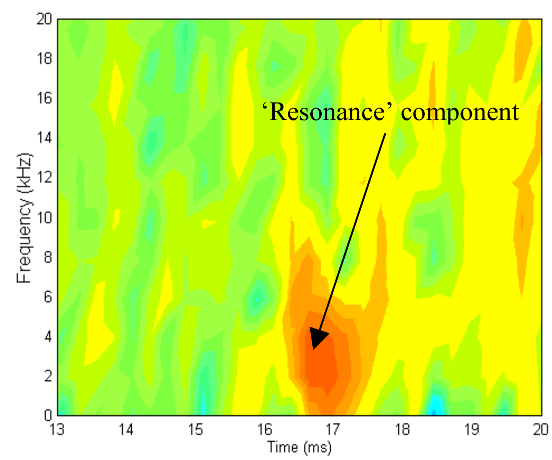

Fig. 8. Narrow-band spectrogram for target insonification by 7 kHz Ricker signal: free-field, -4^0 aspect angle.

Ricker signal. This can be compared with Fig. 8, for the response of the target in a similar orientation in the free field. The strongest return is seen in both cases between 3 and 7 kHz, slightly lagging the specular return from the front face of the target that shows prominently in Fig. 6. This return appears to be one or more low-frequency resonances of the target and is clearly an important classification parameter. Comparison of Figs 6 and 8 show that the resonances are of shorter duration for the embedded target, probably due to the damping effects of the surrounding sediment. Comparison of the results for the target *present/not present* suggests that most of the lower frequency energy components visible in Figs 6 and 7 are due to the presence of the target.

Fig. 9 shows the 7 kHz Ricker target response for a $+10^0$ aspect angle at a grazing angle of 40^0. Some similarities in the echo structure with that of the near broadside position shown in Fig 6 are evident. The specular echo from the front face is less prominent, and the majority of the energy is returned in the range 2-8 kHz, corresponding to similar components shown in Figs 6 and 7. Again, this component

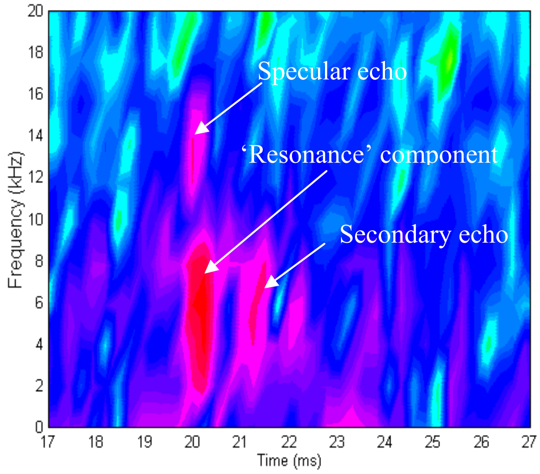

Fig. 9. Narrow-band spectrogram for target insonification by 7 kHz Ricker signal: 40^0 grazing angle, $+10^0$ aspect angle.

may be due to a combination of resonance effects. A secondary echo, approximately 1.18 ms after the main resonance echo, is also evident. This echo was also observed in the near-broadside position but at a lower intensity relative to the main resonance and specular returns. The source of the secondary echo is not fully understood.

Both time and frequency domain analysis of aspect angles greater than $\pm 26^0$ showed a poor signal-to-noise ratio for returned signals, making identification of the target echo components difficult. Analysis of signals for the end-cap aspect also proved difficult.

CONCLUSIONS

Experiments were carried out in the sea with a parametric sonar system to provide data representing the acoustic response of a thin-walled, water-filled cylinder with flat end-caps. The cylinder was insonified, at a range of grazing angles and aspect angles, whilst partially embedded in soft sediment. Analysis of direct and target-scattered signals showed that target detection was possible for aspect angles up to 23^0 from the broadside position and for seabed grazing angles from 32^0 to 42^0. Comparison of target *present / not-present* data also gave good evidence of the detection of target-generated, back-scattered components in the 1-20 kHz frequency range. Comparison with free-field data for similar signal types and target orientations showed a reasonable correlation in observed echo structure, including the identification of front-face specular returns up to 10^0 from broadside and possible low frequency resonance components up to 23^0 from broadside. Analysis of seabed reverberation levels at 1-20 kHz showed little or no significant back-scattered energy from the sediment with the target removed, due to penetration and absorption of the signal. This was compared with the high reverberation levels observed with the 75 kHz 'primary' frequency, making target detection difficult.

The results showed that a parametric source appears to be a viable option for the detection and possible classification of seabed-embedded targets. The advantage of such a source was that effects could be observed both at high frequencies (at the 'primary' frequency of 75 kHz) and at low frequencies (typically less than 20 kHz, corresponding to 'secondary' frequencies). Some degree of target classification using relatively simple analysis techniques was possible from measurement of front and back face specular returns, for a relatively narrow band of target aspect angles. The observation of low frequency resonance effects is also promising as a means of providing additional data for classification.

Acknowledgments

The research presented here has depended on a team effort, for which the authors thank Paul Connelly, Jim Cook, Dave Goodson, Darryl Newborough and Chris Richards (Loughborough University); Eric Armstrong, Phil Copland and John Simmonds (Marine Fisheries Laboratory, Fisheries Research Services, The Scottish Office); Tom Curtis and Any Webb (Defence Evaluation and Research Agency); Mike Somers (Institute of Oceanographic Sciences Deacon Laboratory); and many colleagues from Thomson Marconi Sonar (France), TNO-FEL (The Netherlands), and the University of Genoa, Alenia-Whitehead and SACLANT Centre (Italy), who participated in the European Commission MAST-III DEO project.

REFERENCES

[1] R. Lim, J.L. Lopes, R.H. Hackman, and D.G. Todoroff, "Scattering by objects buried in underwater sediments: theory and experiments," *J.Acoust.Soc.Am.*, vol. 93, no. 4, pp. 1762-1783, 1993.

[2] J.C. Cook, A.D. Goodson, P.A. Lepper, and B. Woodward, "The design and evaluation of a phase-steered parametric sonar system intended for sediment characterisation," *J. Soc. Underwater Technology*, vol. 22, no. 2, pp. 43-54, 1997.

[3] R. Guillermin, J.P. Sessarego, and J. Sageloli, "Characterization of buried objects in marine sediments," *Proc. IEEE Oceans '98*, vol. 1, pp. 18-21, 1998.

[4] M. Gensane, S. Fioravanti, M. Granara, J.C. Sabel, A. Tesei, M. Tran Van Nhieu, A. Trucco, and B Woodward, "Detection of Embedded Objects (DEO)," *Proc. Third European Marine Science and Technology Conference*, Lisbon, pp. 1140-1153, 1998.

[5] P.A. Lepper, *The Development and Testing of a Parametric Sonar System for Use in Sediment Classification and the Detection of Buried Objects*, Ph.D. Thesis, Loughborough University, U.K., October 1999.